



HAL
open science

Alterations of tactile and anatomical spatial representations of the hand after stroke

Lucile Dupin, Eloïse Gerardin, Maxime Térémetz, Sonia Hamdoun, Guillaume Turc, Marc Maier, Jean-Claude Baron, Pålvel Lindberg

► **To cite this version:**

Lucile Dupin, Eloïse Gerardin, Maxime Térémetz, Sonia Hamdoun, Guillaume Turc, et al.. Alterations of tactile and anatomical spatial representations of the hand after stroke. *Cortex*, 2024, 177, pp.68-83. 10.1016/j.cortex.2024.04.015 . hal-04801676

HAL Id: hal-04801676

<https://hal.science/hal-04801676v1>

Submitted on 25 Nov 2024

HAL is a multi-disciplinary open access archive for the deposit and dissemination of scientific research documents, whether they are published or not. The documents may come from teaching and research institutions in France or abroad, or from public or private research centers.

L'archive ouverte pluridisciplinaire **HAL**, est destinée au dépôt et à la diffusion de documents scientifiques de niveau recherche, publiés ou non, émanant des établissements d'enseignement et de recherche français ou étrangers, des laboratoires publics ou privés.



Distributed under a Creative Commons Attribution - NonCommercial 4.0 International License



Special Issue “From Bodies to Spaces: a neurocognitive/neuropsychological perspective”

Alterations of tactile and anatomical spatial representations of the hand after stroke



Lucile Dupin ^{a,b,*}, Eloïse Gerardin ^{a,1}, Maxime Térémetz ^{a,1},
Sonia Hamdoun ^{a,c}, Guillaume Turc ^{a,d}, Marc A. Maier ^b,
Jean-Claude Baron ^{a,d} and Pålvel G. Lindberg ^a

^a Université Paris Cité, Institute of Psychiatry and Neuroscience of Paris (IPNP), INSERM U1266, F-75014 Paris, France

^b Université Paris Cité, INCC UMR 8002, CNRS, F-75006 Paris, France

^c Service de Médecine Physique et de Réadaptation, GHU-Paris Psychiatrie et Neurosciences, Hôpital Sainte Anne, F-75014 Paris, France

^d Department of Neurology, GHU-Paris Psychiatrie et Neurosciences, FHU Neurovasc, Paris, France

ARTICLE INFO

Article history:

Received 28 November 2023

Reviewed 6 February 2024

Revised 19 March 2024

Accepted 18 April 2024

Published online 21 May 2024

Keywords:

Body representation

Spatial coding of touch

Tactile remapping

Stroke

Hemiparesis

ABSTRACT

Stroke often causes long-term motor and somatosensory impairments. Motor planning and tactile perception rely on spatial body representations. However, the link between altered spatial body representations, motor deficit and tactile spatial coding remains unclear. This study investigates the relationship between motor deficits and alterations of anatomical (body) and tactile spatial representations of the hand in 20 post-stroke patients with upper limb hemiparesis. Anatomical and tactile spatial representations were assessed from 10 targets (nails and knuckles) respectively cued verbally by their anatomical name or using tactile stimulations. Two distance metrics (hand width and finger length) and two structural measures (relative organization of targets positions and angular deviation of fingers from their physical posture) were computed and compared to clinical assessments, normative data and lesions sites. Over half of the patients had altered anatomical and/or tactile spatial representations. Metrics of tactile and anatomical representations showed common variations, where a wider hand representation was linked to more severe motor deficits. In contrast, alterations in structural measures were not concomitantly observed in tactile and anatomical representations and did not correlate with clinical assessments. Finally, a preliminary analysis showed that specific alterations in tactile structural measures were associated with dorsolateral prefrontal stroke lesions. This study reveals shared and distinct characteristics of anatomical and tactile hand spatial representations, reflecting different mechanisms that can be affected differently after stroke: metrics and

* Corresponding author. 45 Rue des Saints-Pères, 75006 Paris, France.

E-mail address: lucile.dupin@cnrs.fr (L. Dupin).

¹ Contributed equally.

<https://doi.org/10.1016/j.cortex.2024.04.015>

0010-9452/© 2024 The Author(s). Published by Elsevier Ltd. This is an open access article under the CC BY-NC license (<http://creativecommons.org/licenses/by-nc/4.0/>).

location of tactile and anatomical representations were partially shared while the structural measures of tactile and anatomical representations had distinct characteristics.

© 2024 The Author(s). Published by Elsevier Ltd. This is an open access article under the CC BY-NC license (<http://creativecommons.org/licenses/by-nc/4.0/>).

1. Introduction

Knowing the location of each part of the body is a prerequisite for planning movement trajectories and to execute body movements (Cohen & Andersen, 2002). For instance, the hand and finger trajectories for grasping an object depend on their initial location, i.e., on their spatial representation. Accurate spatial representation of the body is also necessary for defining the spatial characteristics of tactile information, such as determining the location of a tactile stimulation, for locating an obstacle or identifying the shape of an object through touch. Indeed, motor function, somatosensation and body representation are functionally linked and interdependent (Brandes & Heed, 2015; Cataldo et al., 2021, 2022, Dupin et al., 2015, 2017, 2018, 2021). This is particularly true for the hand, the primary organ for interaction with and interpretation of the proximal physical world. Manual dexterous movements rely specifically on the interaction between motor and somatosensory functions.

After stroke, motor deficits of the upper limb are frequently observed compromising hand function (Plantin et al., 2021; Ramsey et al., 2017). Tactile deficits and their recovery have been found to occur concomitantly with motor deficits (Meyer et al., 2014, 2016; Zandvliet et al., 2020). For instance, alterations in tactile detection and discrimination correlate with motor deficits, while recovery of motor and tactile deficits occur in parallel (Zandvliet et al., 2020). The dissociation between the functions of locating the anatomical and tactile targets introduced the concepts of “body schema” and “superficial schema” respectively (Head & Holmes, 1911; Longo et al., 2010), was based on observations in stroke patients who were able to locate a tactile stimulation but not the explicit position of the underlying body part, and vice versa. Altered spatial characteristics of hand representations has been described in case reports of stroke patients for touch with erroneous relative localizations and/or shifts in general location (Birznieks et al., 2012; Rapp et al., 2002; Rinderknecht et al., 2019).

However, larger group studies are lacking and little is known on the link between characteristics of spatial representation of the body, touch and motor function, and how their relation may be affected by stroke. In healthy subjects, the spatial hand representation (e.g., implicit body representation from verbal instructions) has long been studied (Haggard et al., 2006; Longo et al., 2015; Longo & Haggard, 2010), and more recently in relation with tactile spatial localization (Dupin et al., 2021; Tamè et al., 2017). Interestingly, metrics and shape of both tactile and implicit body representations from verbal cueing, namely ‘body model’ (Longo &

Haggard, 2010) do not reflect the spatial physical properties of the hand but show systematic distortions such as shorter fingers and larger hand width (Dupin et al., 2021; Tamè et al., 2017; Verbe et al., 2021). However, metrics and shape of spatial hand representations obtained through touch or verbal instructions also differ in several aspects (Dupin et al., 2021; Verbe et al., 2021). These distortions of spatial hand representations are not static over time: recent studies (Dupin et al., 2021; Van der Looven et al., 2021) have shown that they result from a continuous shrinking that starts in childhood and evolves continuously across the lifespan. Furthermore, the spatial hand representation has been found to be affected by long-term training and expertise: hand representations of expert baseball players (Coelho et al., 2019) and experienced sign language interpreters (Mora et al., 2021) show reduced hand width and finger length compared to control subjects. Finally, metric distortions of body representation are commonly observed for perception and action (Peviani & Bottini, 2018).

The fact that the metrics of spatial hand representations could vary may reflect functional, yet still unknown, characteristics of the hand (Caggiano & Cocchini, 2020; Dupin et al., 2021; Medina & Coslett, 2016). Since a correct spatial body representation is necessary for movement planning, and because spatial hand representations evolve with time (Dupin et al., 2021; Van der Looven et al., 2021) and expertise (Coelho et al., 2019; Mora et al., 2021), it seems relevant to understand how these representations are affected in patients with centrally-caused upper limb motor deficits. In fact, hand representation could be affected either functionally due to the motor deficit caused by the lesion or as a directly affected by the lesion. In this latter hypothesis, linking hand representation alterations and lesion site could provide answers. In this study we aim to identify and characterize alterations in tactile and body spatial representations of the hand (from verbal cueing) in stroke patients by assessing the metrics and spatial organization of hand representations based on 10 targets (the finger nail and metacarpophalangeal joint of each finger). The participants, with their eyes closed, were instructed to localize (i.e., to point to) each target cued either by a tactile stimulus applied to the target or by a verbal instruction naming the anatomical target, in order to assess these two spatial representations (see Fig. 1A for experimental set-up and targets). All 20 patients included in this study showed post-stroke upper limb motor deficits (hemiparesis) but did not have severe deficits of tactile light touch detection. Altered representations were i) quantified with respect to normative data from a previous study (Dupin et al., 2021); ii) compared to clinically-assessed post-stroke motor and sensory deficits; and finally iii) used in

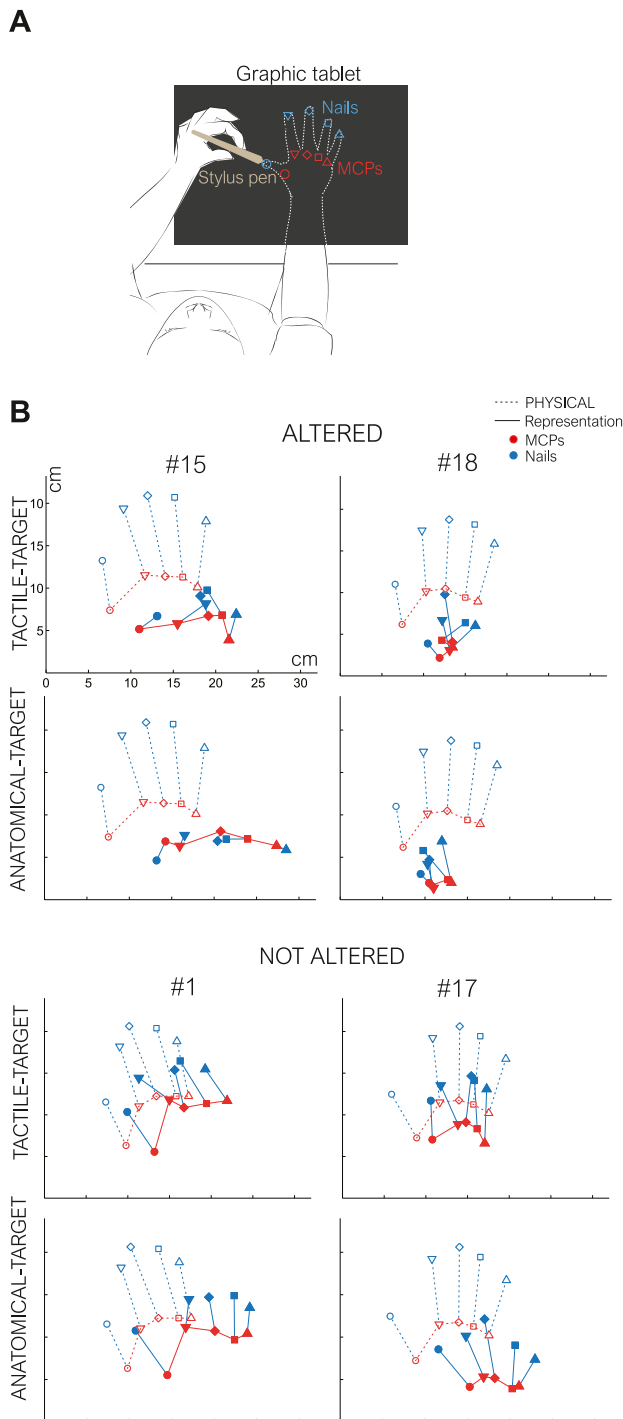


Fig. 1 – Set-up and representative anatomical and tactile spatial representations. **A.** Scheme of the set-up and the 10 targets (MCP in red and nails in blue) assessed in PHYSICAL, TACTILE- and ANATOMICAL-TARGET conditions. The participants used a stylus pen held with the pointing hand to indicate, without vision, where he/she located the targets (position of a particular finger nail or of a MCP joint) on a graphic tablet positioned over the target hand. **B.** Spatial representations of the paretic hand of four representative participants. Top: patients #15 and #18 with altered representations (see Tables 2 and 3), and

MRI-based lesion-symptom mapping in order to explore the cerebral substrates of these deficits.

2. Material & methods

2.1. Participants

Twenty patients (5 females/15 males, age >18 years, mean age \pm SD: 56.9 ± 16.6 years) were recruited from the Dextrin randomized rehabilitation trial at the GHU Psychiatrie et Neurosciences hospital (trial number NCT03934073). Sample size was similar to groups size in a previous study (Dupin et al., 2021). Inclusion criteria included: first-symptomatic ischemic or hemorrhagic stroke with upper-limb hemiparesis and in the chronic phase (>3 months post-stroke). All patients (>18 years old) had mild-to-moderate hand motor impairment, indicated by Box and Blocks Test (BBT) score <52 blocks/minute and ≥ 1 block and 10° active extension of the wrist and index metacarpophalangeal joint. Included patients had a single stroke, no neglect, and mild-to-moderate tactile impairments. Exclusion criteria: cognitive impairment [i.e., Mini Mental State Examination (MMSE) score < 25], presence of botulinum toxin treatment to spastic muscles of the upper limb <3 months before inclusion or planned during the protocol. Written informed consent was obtained before the experiment and the study was approved by the regional ethics committee (CPP 2018-A01945-50) and complied with the Declaration of Helsinki. No part of the study procedures was pre-registered prior to the research being conducted. We report how we determined our sample size, all data exclusions, all inclusion/exclusion criteria, whether inclusion/exclusion criteria were established prior to data analysis, all manipulations, and all measures in the study. No part of the study procedures or analysis plans was preregistered prior to the research being conducted.

2.2. Clinical assessments

Five clinical assessments were used in order to evaluate upper limb motor functions: Motor activity Log (MAL, Taub et al., 1993), Box and Block Test (BBT, Mathiowetz et al., 1985), Action Research Arm Test (ARAT, Lyle, 1981), Moberg Pick-Up test (MPUT, Moberg, 1958) and maximum grip force assessed using dynamometer. Somatosensory (tactile) function (light touch of the digits) was assessed using Semmes-Weinstein monofilaments (Weinstein, 1993). MAL is a quantitative and subjective assessment used to evaluate the daily use of the paretic arm involving self-reporting by the patient on the frequency and quality of use of the paretic arm, BBT is used for evaluating gross motor function of the hand and arm,

bottom patients #1 and #17 without alterations in TACTILE- and ANATOMICAL-TARGET conditions (continuous lines/filled markers) compared to the PHYSICAL hand (dashed lines/empty markers). Finger length and nails are represented in blue and MCPs in red. The two targets for each finger are represented by the same symbol (e.g., circle for the thumb, for other fingers see panel A).

involving to move blocks from one side of a box to another within a set time, ARAT is an assessment tool used to evaluate upper limb function in specific tasks involving reaching, grasping and manipulating objects, MPUT assessed fine/dexterous movements of the hand using tasks that require precise control and coordination of finger movements.

Demographic and clinical data are detailed in Table 1. In order to avoid ceiling effects, we excluded the ARAT score from analyses since only 5 (of 20) patients were slightly lower than maximum score (57).

2.3. Tactile and anatomical spatial representation of the hand

2.3.1. Apparatus

The device for quantifying the spatial representation of the (immobile) hand (Fig. 1A; Dupin et al., 2021) consisted of a graphic tablet (HUION WH1409) connected to a PC through USB. The graphic tablet was mounted on a support by means of two slides so that the tablet could slide away from the target hand in order to locate the physical position of the target (resting) hand and fingers. Data acquisition software was developed in C++. Digital study materials are available at <https://doi.org/10.17632/yzp6vkzt29.1>.

2.3.2. Task

The aim of the task was to assess the location of 10 targets for each hand: the position of the 5 finger nails and the 5 metacarpophalangeal joints (MCP) (Fig. 1A.) in 2 different conditions: TACTILE, cued through tactile stimulations, and ANATOMICAL-TARGET cued through verbal instructions (Dupin et al., 2021; Longo & Haggard, 2010) described below. We also assessed the physical location of each target (PHYSICAL).

For each participant, the ANATOMICAL-TARGET and TACTILE-TARGET conditions were presented in a random order but this order was the same for the two hands of a given participant. The order of the two hands was randomized between participants. No feedback of task performance (pointing error) was provided. Before the beginning of the experiment, we ensured that all patients were able to recognize and show their fingers based on verbal instruction (no autotopagnosia/finger agnosia).

2.3.3. Procedure

Participants sat on a chair with armrest. The armrest of the target hand was aligned with the center of the device so that the target hand was positioned in the axis of the shoulder (Fig. 1A). The target hand was placed in the device (under the graphic tablet), palm down with the fingers abducted. However, for some participants with spasticity, finger abduction had to be reduced. The experimenter ensured that the position of the target hand was sufficiently comfortable for the participant to maintain this resting position without effort. Participants were instructed to not move the target hand and keep it relaxed during all testing conditions that lasted, all together, about 30 min. After assessing the PHYSICAL location of each target, the participant used his/her pointing hand to indicate the instructed target position with the stylus pen on the tablet, without vision (eyes closed). Typically, the stylus pen was held in a precision grip, but when using the paretic hand, some

participants used a whole hand grasp. The paretic and non-paretic hand served successively as target hand (and respectively as pointing hand, in randomized order between participants).

2.3.4. Conditions

2.3.4.1. PHYSICAL CONDITION. The aim was to record the physical position of the 10 targets defining the spatial configuration of the hand and fingers. To record a given target, the graphic tablet was slid away from the hand so that the hand was visible. A laser pointer was positioned vertically pointing directly to the target to be measured. Then the tablet was moved to the closed position and the luminous point of the laser was recorded using the stylus pen of the graphic tablet. Each target was recorded once. In order to take into account possible involuntary movements of the target hand the PHYSICAL target points were measured at the beginning and at the end of the testing of each hand.

2.3.4.2. TACTILE-TARGET CONDITION. The participant kept the eyes closed during the entire condition. In a given trial, the experimenter touched the participant at one of the 10 possible targets. The participant then had to position the stylus pen directly above the perceived tactile stimulation. The tactile stimulation consisted of a continuous steady pressure applied on the target by means of pencil equipped with a rubber pad. The tactile stimulation lasted until the participant validated verbally his/her response. The order of the targets was randomized and each of the 10 targets was repeated 3 times (30 trials for each hand).

2.3.4.3. ANATOMICAL-TARGET CONDITION. The task body spatial representation assessment (Longo & Haggard, 2010) was similar to TACTILE-TARGET condition, except that the experimenter indicated the anatomical name of the target verbally before each trial: a finger nail or MCP joint of a given finger (for example: “joint of the index finger”, in French in the experiment).

2.4. Data computation

For each hand and condition, we computed two metrics and two structural measures of the hand representation in order to quantify its potential distortion. Behavioral data are available at <https://doi.org/10.17632/yzp6vkzt29.1>.

The study adheres to the General Data Protection Regulation (GDPR), in accordance with European legislation. Imaging data may be shared upon request to the corresponding author, provided it complies with GDPR and the local ethics committee rules.

2.4.1. Two metrics: finger length and hand width

We computed the two usual metrics in spatial hand representation: hand width and finger length. Hand width was determined as the sum of the four successive distances between the MCP joints from finger I (thumb) to V (little finger). To determine the mean finger length, the individual length of each finger (from MCP to its nail) was computed and averaged over the 5 fingers.

Table 1 – Demographic and clinical information for each patient: age, stroke type, side of impaired limb and scores for clinical motor and sensory assessments.

Patient #	Age (years)	Type of stroke (I: ischemic, H: hemorrhagic)	Side of impaired upper limb	MPUT impaired limb (mean time for 1 element/s)	MPUT non impaired limb (mean time for 1 element/s)	Force max. Impaired limb (% of non- impaired)	Force max. Non impaired limb (N)	BBT (number cubes/min)	MAL (AOS/QOM) (0–5/0–5)	ARAT (0–57)	Light touch: Impaired limb (0–50)	Light touch: Non impaired limb (0–50)	Delay between stroke and clinical assessments (months)	Delay between stroke and hand/ representation assessments (months)
1 ^b	25	I	R	6	1.13	62.2	37	26	1.8/1.56	57	50	50	24	24
2	43	I	R	1.25	1.08	91.7	24	49	2.86/2.76	57	50	50	10	24
3 ^b	40	I	R	1.96	1.13	95.4	43	37	2.82/2.42	57	50	50	6	7
4	45	I	L	2	1.38	52.7	55	45	3/2.82	57	35	45	12	17
5	77	I	R	3.75	1.08	67.7	34	48	1.84/1.26	57	18	40	6	7
6 ^b	57	H	L	3.5	1	80.0	50	46	1.78/1.86	57	40	50	29	42
7 ^b	34	I	R	12	1.04	26.7	45	17	1.1/1.16	54	50	50	46	50
8	53	H	R	1.58	1.33	111.4	35	39	2.1/2.2	57	50	50	52	65
9 ^b	91	I	L	4.92	2	46.7	30	26	1.14/1.22	57	50	50	8	7
10	74	I	L	1.58	1.08	65.0	20	41	2.56/2.24	57	45	40	5	6
11 ^b	63	I	R	1.33	1.33	58.3	36	65	2.48/2.26	57	40	40	3	16
12 ^b	72	I	L	4.17	1.5	65.4	26	30	.96/.94	52	35	40	5	5
13	73	H	L	4.17	1.46	46.7	45	21	1/9/1.72	55	10	50	14	12
14	75	I	R	1.25	.92	51.7	29	50	1.9/1.72	57	36	45	3	5
15 ^b	44	I	R	4	1.25	34.0	50	31	.74/.64	49	38	40	59	61
16	65	I	R	6.7	1	67.4	49	28	1.3/1.32	57	44	44	18	29
17 ^b	59	I	R	8.57	.83	82.1	28	21	1.02/1.08	47	40	40	117	130
18	60	I	R	2	1	83.3	30	44	2.04/2.02	57	48	50	34	19
19	46	I	R	1.67	.83	89.3	28	55	2.96/2.9	57	50	50	14	40
20	41	I	R	1.08	1	93.8	32	29	1.3/1.4	57	44	44	9	9
Mean ± SD	56.9 ± 16.6	3 H 17 I	6 L 14 R	3.7 ^a ± 2.8	1.2 ± .3	68.6 ^a ± 22.1	36.2 ± 9.8	37.4 ± 12.5	1.87/1.81 ± .73/ .66	55.6 ± 2.9	41.2 ± 10.6	45.9 ± 4.4	29.5 ± 29.5	23 ± 26.9

MPUT for Moberg Pick-Up test, BBT for Box and Block Test, MAL for Motor Activity Log, ARAT for Action Research Arm Test.

^a Corresponds to a significant difference between paretic and non-paretic arm (paired t-test).

^b Patient underwent MRI.

In order to avoid potential confounding effects of different inter-individual physical hand size, hand width and finger length from TACTILE- and ANATOMICAL-TARGET conditions were normalized, i.e., divided, by the PHYSICAL measure of the hand (for hand width and finger length). Consequently, a normalized value <1 indicates a smaller representation of the hand relative to its physical size.

2.4.2. Two measurements of spatial structure: organization & angular deviation

2.4.2.1. ORGANIZATION SCORE. The organization score quantifies the general spatial organization of the 10 targets (nails and MCPs). This score is the combination of 2 subscores:

Subscore_1: The relative organization of the successive MCP target and the successive nails, computed on the x (longitudinal) axis. For instance, the MCP of the thumb of the right hand should be positioned on the left of the MCP of the index finger. There were 4 comparisons for MCP, plus 4 for nails. For each comparison, a binary value of 1 = correct relative position or 0 = inverted relative position was attributed.

Subscore_2: Fingertip intrinsic organization: This second subscore quantifies the number of correct relative locations between the fingertips and the corresponding MCP on the y axis. For instance, the MCP of one finger should be positioned more proximally (lower y value) than its fingertip (nail). For each finger, a binary value was attributed: 1 = correct, 0 = incorrect relative position.

The sum of the 2 subscores was multiplied by 100 and divided by 13 (total number of comparisons) in order to obtain a percentage value (100% corresponds to correct relative spatial organization, and 0% indicates that none of the 13 relative target positions were correct).

2.4.2.2. ANGULAR DISTORTION. Finger angular distortion corresponds to the angular difference between a given physical finger and its corresponding representation in the TACTILE- or ANATOMICAL-TARGET condition. To compute this distortion, the orientation of each finger was defined as a vector between MCP and its nail, and the angular distortion computed from the scalar product of the two vectors.

In the PHYSICAL condition, the vector of one finger PHY [PHY_x, PHY_y] was defined between the MCP coordinates [MCP_x, MCP_y] and NAIL coordinates [$NAIL_x, NAIL_y$] as [$NAIL_x - MCP_x, NAIL_y - MCP_y$]. Similarly in TACTILE- and ANATOMICAL-TARGET conditions, the vector for the representation of the corresponding finger REP [REP_x, REP_y] was defined based as [$NAIL_x - MCP_x, NAIL_y - MCP_y$].

The angular distortion θ was then computed as:

$$\theta = \cos^{-1}(\frac{PHY_x REP_x + PHY_y REP_y}{\|PHY\| \cdot \|REP\|})$$

2.4.3. Localization

The localization of hand representation was computed as the barycenter of the 10 targets. Localization of nails as the barycenter of the 5 targets corresponding to nails and similarly for MCPs.

2.4.4. Normative values

Normative data were computed from 60 healthy participants (30 female/30 male, aged 20–79 years) from a previous study (Dupin et al., 2021). They declared having no hand motor deficit due to local trauma or central neurological disease, no disease potentially affecting sensory functions (such as diabetes) and no psychiatric disorder. We used their mean \pm 2 SD values (of the non-dominant target hand) as cut-off values for altered representations.

2.4.5. Magnetic resonance imaging (MRI)

Due to COVID-related factors and inclusion criteria, only nine out of the 20 patients underwent T1 MRI scans (Table 1). MRI data were collected on a 3T MRI (Canon) with a 12-channel head-coil. Anatomical MRI consisted of a high-resolution axial 3D inversion recovery T1-weighted sequence (matrix 384 × 384, FOV 25 cm, slice thickness 1.2 mm, 140 slices, TE/TI/TR 4.3/400/11.2 msec, acquisition time 6.07 min).

Anatomical T1 images underwent normalization to the Montreal Neurological Institute template via the SPM12 software package (<https://www.fil.ion.ucl.ac.uk/spm/software/spm12/>). Manual delineation of lesion maps was performed across all axial slices of native space T1-weighted anatomical images, a process carried out by P.L. (blinded to clinical and behavioral assessments) using MRICron (<https://people.cas.sc.edu/rorden/mricron>). Where accessible, lesion localization was cross-referenced and confirmed against FLAIR images, leading to the creation of binarized lesion maps. Lesion figures were generated using MRICronGL v1.2 (<https://github.com/rordenlab/MRICroGL>).

2.5. Statistical analyses

The normality of the data was tested using the Shapiro–Wilk test. To compare non normal data, we used Wilcoxon signed-rank or Kruskal–Wallis tests for independent samples instead of t-tests.

2.5.1. Correlations and corrections

We used Pearson correlations for quantifying relations between variables. Since *hand width* and *finger length* can be affected by age, the relation between scores of clinical motor assessments and metrics of hand representation was computed using partial correlations controlled for age effect.

All correlations were corrected for multiple comparisons using a correction for non-independent samples (Cheverud, 2001; Derringer, 2018; Nyholt, 2004). The threshold for significance $\alpha \times Meff$ resulting from this correction is indicated after the *p*-value of each test and was defined as: $Meff = 1 + [(k - 1) \times (1 - \text{var}(\lambda) k)]$, with λ defined as the vector of eigenvalues of length *k* where total family-wise error rate $\alpha = .05$. This resulted in an adjusted significance threshold of .0117.

2.5.2. Atlas-based lesion-symptom mapping analysis

We used Atlas-based Lesion-Symptom mapping (LSM) approach using statistical lesion analysis software NiiStat (<https://github.com/neurolabusc/NiiStat>). This method is based on the cumulative lesion load within a designated ROI (Region of interest, atlas-based), rather than examining

lesions voxel by voxel. Cluster-level family-wise error correction via permutation testing was set to 10,000 permutations at $p > .05$. Atlases used for LSM were Brodmann areas (based on their cytoarchitecture) (Brodmann, 1909) and JHU tractography atlas for white-matter (Mori & Crain, 2005; Wakana et al., 2007). Only regions where lesions were present in at least 20% of the patients were incorporated into the analysis ($n \geq 2$). Based on this criterion, 19 of 82 regions were selected for Brodmann atlas and 53 of 189 for JHU atlas. To assess the statistical robustness, we also performed the investigation for $n \geq 3$, representing 33% of participants with voxels containing lesions within the targeted region. Based on this criterion, 7 of 82 regions were selected for Brodmann atlas and 32 of 189 for JHU atlas. All correlations have been controlled with more conservative Bonferroni correction.

3. Results

3.1. Characteristics of the representations of the paretic hand

Demographic and clinical information for each patient are described in Table 1. Tables 2 and 3 present the individual values of the 4 quantitative variables (*Hand width*, *Finger Length*, *Organization score* and *finger angular deviations*) of hand representations for the TACTILE- and ANATOMICAL-TARGET conditions. Overall, 13 and 9 patients showed at least one significantly impaired variable with the TACTILE- and ANATOMICAL-TARGET conditions, respectively. All individual spatial hand representations are available in Supplementary Fig. S1. Two participants (#15 and #18) presented in Fig. 1B showed impaired representations in both TACTILE- and ANATOMICAL-TARGET conditions (see Tables 2 and 3 for details), while other participants (#1 or 17) did not show any values outside the normative range. The hand representations for these 4 participants in the TACTILE- and ANATOMICAL-TARGET conditions are illustrated in Fig. 1B, which shows a wide inter-individual variability.

3.1.1. Comparison between the TACTILE- and ANATOMICAL-TARGET conditions

For the paretic hand, *Hand width* and *Finger length* correlated significantly between the two conditions (*Hand width*: $r = .52$, $p = .023$; *Finger length*: $r = .60$, $p = .007$, partial correlation controlled for age), indicating that the extent of the verbally induced and the tactile-induced spatial representations appear to be related (independently from age). However, this was not the case for *Organization score* and *Angular distortion*: these measures did not correlate between conditions (*Organization score*: $r = .19$, $p = .44$, and *Angular distortion*: $r = .14$, $p = .57$, controlled for age).

3.1.2. Comparison between paretic and non-paretic hand

In order to identify whether the representation of the paretic hand showed specific alterations, we compared the spatial characteristics between the affected and non-paretic hand. Only *Organization score* in the ANATOMICAL-TARGET condition was significantly different between the two hands

($p = .004$, sign-test). A third of patients (7/20) showed at least one score of the non-paretic hand outside the normal range, but more than half (13/20) had at least one abnormal value in the paretic hand (in the TACTILE-TARGET condition, see Table 2). Similarly, in the ANATOMICAL-TARGET condition, fewer patients (6/20) had values beyond the cut-off for the non-paretic compared to the paretic hand (9/20, Table 3).

Furthermore, we investigated whether the different metrics and structural measures correlated between hands, which may indicate shared (intra-subject) characteristics of pathologic distortions. In the TACTILE-TARGET condition, *Finger length* correlated between hands ($r = .50$, $p = .029$, partial correlation controlled for age), but not *Hand Width* ($r = .26$, $p = .29$, controlled for age). Conversely, in healthy participants, both metrics strongly correlated between hands (Pearson $r = .59$, $p < .00001$ and $r = .71$, $p < .00001$ for *finger length* and *hand width*, respectively (Dupin et al., 2021)), indicating partial dissociation between the representation of the two hands after stroke. *Organization score* and *Angular distortion* in TACTILE-TARGET condition did not correlate between hands (all $r < .40$, $p > .08$). In the ANATOMICAL-TARGET condition, both *Hand Width* and *Finger length* correlated between hands ($r = .50$, $p = .028$ and $r = .59$, $p = .007$, respectively, controlled for age). Moreover, *Organization score* and *Angular distortion* also significantly correlated between hands ($r = .67$, $p = .002$ and $r = .90$, $p < .001$, respectively).

Thus, the non-paretic hand appeared to share some characteristics of the representation of the paretic hand in both the TACTILE- and ANATOMICAL-TARGET conditions.

3.1.3. Comparison between right and left hemisphere lesions

In order to identify asymmetry between left and right hemisphere lesions, we compared the different measures between these two subgroups ($n = 14$ for the left hemisphere and $n = 6$ for the right hemisphere). No significant difference was found (all $X^2 < 2.46$, $p > .11$, Kruskal–Wallis).

3.2. Relation with clinical motor assessments (Paretic Hand)

3.2.1. Hand width

Hand width of the paretic hand in the TACTILE-TARGET condition, controlled for age, correlated significantly and positively with MPUT ($r = .68$, $p = .002$, Fig. 2A) and negatively with MAL AOS ($r = -.64$, $p = .003$) and MAL QOM ($r = -.64$, $p = .003$, Fig. 2B). In the ANATOMICAL-TARGET condition, *Hand width* correlated negatively with BBT ($r = -.57$, $p = .01$). A greater MPUT score indicates lower motor performance, while in MAL and BBT a lower score corresponds to lower performance. Thus, the above correlations consistently indicate that a larger hand width relates to worse motor performance.

3.2.2. Finger length

In the TACTILE-TARGET condition, *Finger length* of the paretic hand, corrected for age, correlated positively with MPUT ($r = .71$, $p = .001$, Fig. 2A). A negative trend with Maximum tap score ($r = -.58$, $p = .02$) was also found. This suggests that longer finger length correlated with poorer motor performances. No significant correlations were found between

Table 2 – Metric and structural values for TACTILE-TARGET condition (hemiparetic upper limb).

Patient #	Paretic limb					Non-paretic limb				
	Hand width	Finger length	Organization	Angular dev.	Nb.	Hand width	Finger length	Organization	Angular dev.	Nb.
1	1.24	.70	100	18.27	0	1.15	.75	100	16.97	0
2	.81	.58	100	14.61	0	.50	.47	100	10.51	0
3	.87	.52	100	7.42	0	1.07	.51	100	26.11 ^x	1
4	.51 ^x	.22 ^x	76.9 ^x	62.16 ^x	4	.94	.90	100	5.18	0
5	.97	.89	92.3 ^x	12.37	1	1.03	.92	100	8.60	0
6	1.04	.72	100	13.97	0	.59	.46	92.3	17.56	0
7	1.64 ^x	1.29 ^x	100	6.95	2	1.12	1.27 ^x	100	7.86	1
8	.85	.26 ^x	84.6 ^x	52.92 ^x	3	.70	.30 ^x	76.9	45.49 ^x	2
9	.83	.60	84.6 ^x	45.66 ^x	2	.62	.33 ^x	76.9	46.61 ^x	2
10	.54 ^x	.33	92.3 ^x	28.26 ^x	3	1.70 ^x	.62	84.6	26.46 ^x	2
11	.55 ^x	.52	92.3 ^x	14.61	2	.56	.54	100	13.00	0
12	1.34	.50	100	6.62	0	1.26	.54	100	17.55	0
13	.57	.21 ^x	61.5 ^x	98.56 ^x	3	.91	.56	92.3	24.86 ^x	1
14	.45 ^x	.36	84.6 ^x	14.42	2	.72	.35 ^x	69.2 ^x	46.41 ^x	3
15	1.14	.39	92.3 ^x	35.67 ^x	2	.94	.74	92.3	16.33	0
16	1.34	.60	92.3 ^x	15.34	1	1.37	.87	100	10.70	0
17	.73	.74	100	15.13	0	.66	.82	100	6.94	0
18	.55 ^x	.52	92.3 ^x	25.70 ^x	3	1.28	.54	100	6.27	0
19	1.00	.66	100	10.66	0	.73	.72	100	13.69	0
20	.72	.40	92.3 ^x	17.20	1	.82	.97	100	12.14	0
Mean ± SD	.88 ± .32	.55 ± .25	91.9 ± 9.6	25.83 ± 22.58	1.5 ± 1.3	.93 ± .31	.66 ± .24	94.2 ± 9.4	18.96 ± 12.95	.6 ± .9
Normative value [mean – 2SD; mean + 2SD]	[.56; 1.37]	[.31; 1.13]	>92.9	[0; 25.1]		[.43; 1.56]	[.36; 1.09]	>90.6	[1.21; 24.73]	

Values followed by ^x indicate individual values outside the normative range for hand width, finger length, organization score and angular distortion. Nb. rows correspond to the number of values outside the normative range for paretic and non-paretic limb.

Table 3 – Metric and structural values for ANATOMICAL-TARGET condition.

Patient #	Paretic limb					Non-paretic limb				
	Hand width	Finger length	Organization	Angular dev.	Nb.	Hand width	Finger length	Organization	Angular dev.	Nb.
1	1.21	.62	100	15.88	0	1.16	.86	100	12.10	0
2	1.26	.58	100	15.74	0	.81	.41	100	25.84	0
3	.73	.71	100	12.76	0	.75	.48	100	8.98	0
4	.76	.62	92.3	20.96	0	.82	.76	100	8.19	0
5	1.03	1.10 ^x	100	8.75	1	1.07	.93	100	11.32	0
6	.84	.64	84.6 ^x	15.69	1	.65	.50	92.3	16.84	0
7	1.51	.92	100	15.90	0	1.19	.46	100	13.11	0
8	1.45	.60	84.6 ^x	32.92	1	.61	.49	92.3	29.59	0
9	1.08	.83	100	11.77	0	1.09	.69	100	20.61	0
10	.69	.48	84.6 ^x	20.53	1	1.23	.75	100	25.87	0
11	.46	.53	100	11.34	0	.42 ^x	.57	100	4.78	1
12	1.51	.12 ^x	61.5 ^x	97.67 ^x	4	1.82	.38	76.9 ^x	59.75 ^x	2
13	2.05 ^x	.45	76.9 ^x	37.78	2	1.04	.54	84.6 ^x	34.68	1
14	.38 ^x	.31	38.5 ^x	15.25	2	.72	.46	92.3	28.76	0
15	1.42	.23 ^x	69.2 ^x	105.85 ^x	3	1.93	.28	76.9 ^x	97.70 ^x	2
16	1.57	.85	92.3	19.67	0	1.97 ^x	.87	92.3	17.58	1
17	.68	.72	100	10.59	0	1.33	.50	100	17.84	0
18	.37 ^x	.45	84.6 ^x	25.66	2	.89	.62	84.6 ^x	42.78 ^x	2
19	1.20	.72	100	21.21	0	1.36	.54	100	13.17	0
20	1.48	.71	92.3	11.19	0	1.18	.70	100	22.36	0
Mean ± SD	1.08 ± .45	.61 ± .23	88.1 ± 15.9	26.35 ± 26.16	.9 ± 1.2	1.10 ± .42	.59 ± .17	94.6 ± 7.7	25.59 ± 20.87	.5 ± .7
Normative value [mean – 2SD; mean + 2SD]	[.45; 1.61]	[.24; 1.08]	>89.3	[0; 39.09]		[.51; 1.86]	[.28; 1.10]	>89.3	[0; 42.46]	

Values followed by ^x indicate individual values outside the normative range for hand width, finger length, organization score and angular distortion. Nb. rows correspond to the number of values outside the normative range for paretic and non-paretic limb.

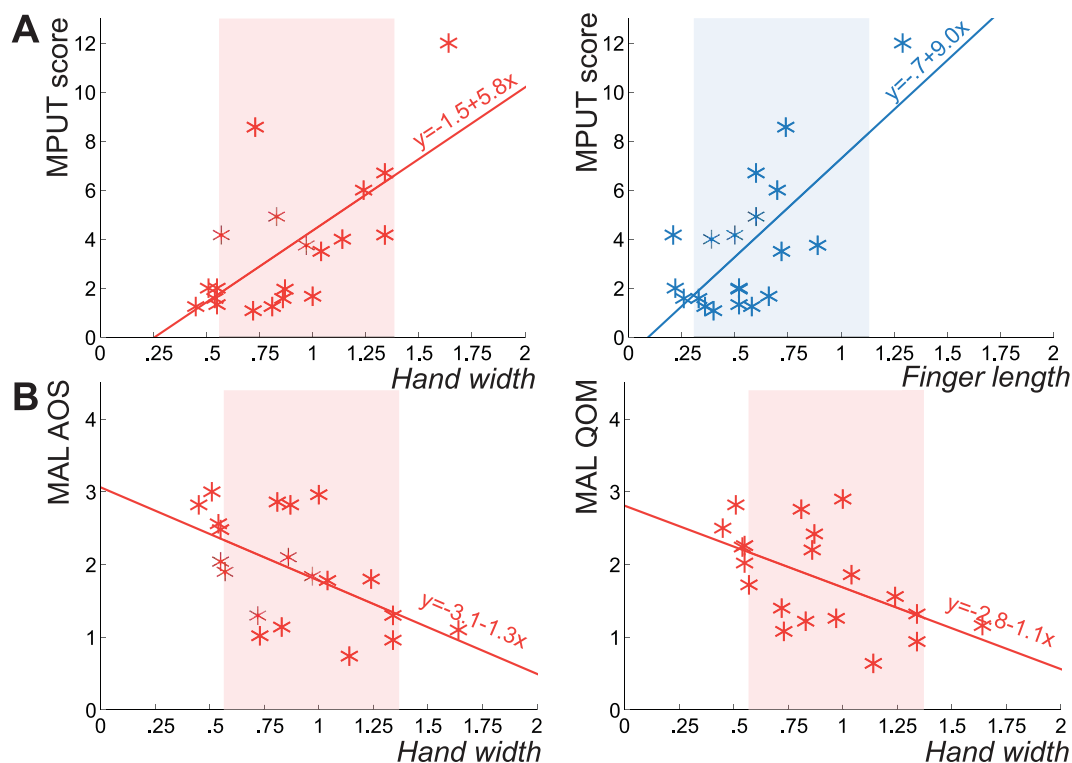


Fig. 2 – Correlations between tactile and anatomical representations and motor assessments. A. Correlations between MPUT score and Hand width (left panel) and Finger length (right panel) in TACTILE-TARGET condition. Red and blue zones correspond to the standard scores in healthy population for Hand width and Finger length respectively. B. Correlations between MAL AOS (left) and MAL QOM (right) and Hand width in TACTILE-TARGET condition.

motor assessments and finger length in the ANATOMICAL-TARGET condition (all $|r| < .36$, $p > .13$).

3.2.3. Organization score and angular distortion

There were no significant correlations between Organization score and motor assessments (all $|r| < .21$, $p > .40$). Likewise, there were no significant correlations between finger Angular distortion score and motor assessments (all $|r| < .44$, $p > .059$).

3.3. Relation with sensory assessment

There were no significant correlations between hand metrics and organization or finger angular distortion and sensory assessments (all $|r| \leq .52$, $p \geq .02$, threshold $p = .0117$). We observed a trend (better tactile function, better organization) with Organization score in the TACTILE-TARGET condition ($r = .52$, $p = .02$).

3.4. Shift in hands localization toward the body

Previous studies reported a shift in tactile localization of targets after stroke (Rapp et al., 2002) toward the body. We analyzed if a specific shift was observed in the hemiparetic stroke group and compared paretic and non-paretic hand.

On the Y-axis (sagittal), both hemiparetic and non-paretic hands exhibit a significant shift toward the body in both the TACTILE-TARGET condition (paretic: mean -4.28 cm,

$t_{19} = -5.98$, $p < .0001$; non-paretic: mean -3.68 cm, $t_{19} = -3.87$, $p = .0001$, t-tests) and the ANATOMICAL-TARGET condition (paretic: mean -4.50 cm, $t_{19} = -7.58$, $p < .0001$; non-paretic: mean -2.87 cm, $t_{19} = -4.06$, $p = .0006$). Sagittal shifts of the paretic and non-paretic hands were not significantly different; only a trend was observed in the ANATOMICAL-TARGET condition ($t_{19} = -1.97$, $p = .06$, paired t-test) and no significant difference in the TACTILE-TARGET condition ($t_{19} = -.67$, $p = .51$, paired t-test).

Nails were more shifted toward the body than MCPs in both TACTILE-TARGET (paretic: means Nails = -6.22 cm, MCPs = -2.34 cm, $t_{19} = 7.92$, $p < .0001$; non-paretic: means Nails = -5.16 cm, MCPs = -2.20 cm, $t_{19} = 6.19$, $p < .0001$) and ANATOMICAL-TARGET conditions (paretic hand: mean Nails = -6.24 cm, MCP = -2.75 cm, $t_{19} = 7.19$, $p < .0001$; non-paretic hand: means Nails = -4.69 cm, MCPs = -1.03 cm, $t_{19} = 9.89$, $p < .0001$). The same pattern was found in control group in TACTILE-TARGET (left hand: Nails = -4.03 cm, MCPs = -1.70 cm, right hand Nails = -5.06 cm, MCPs = -2.84 cm) and ANATOMICAL (left hand: Nails = -4.27 cm, MCPs = -1.43 cm, right hand Nails = -5.33 cm, MCPs = -2.59 cm). Supplementary Fig. 2 illustrates the hands localization shift of the controls and patients and compared ANATOMICAL- and TACTILE-TARGET conditions and left and right hands in patients and control groups.

3.5. Relation to lesion site: atlas-based lesion-symptom mapping

We performed a preliminary atlas-based LSM analysis [due to the limited number ($n = 9$) of participants for whom a MRI was available] to investigate the commonly affected brain regions in impaired tactile spatial coding and body (anatomical) spatial representations. Since only 1 participant had right hemisphere lesion, criterion of analysis (to have at least 2 or 3 patients with overlapping) excluded de facto this patient and so right hemisphere analysis. For each quantified metric and

structural measure of TACTILE- and ANATOMICAL-TARGET representations, we performed the analysis based on Brodmann and JHU atlases.

Fig. 3A and B shows the overlapping lesion sites associated with alterations of the tactile representation of the impaired upper limb assessed in the TACTILE-TARGET condition. All significant LSM results are detailed in Table 4. In the TACTILE-TARGET condition, lesions to Brodmann Area BA32 were correlated with both *Organization score* and *Angular deviation*. Lesions to BA9 and BA46, both mapping to the dorsolateral prefrontal cortex (left), were associated with *Angular deviation*.

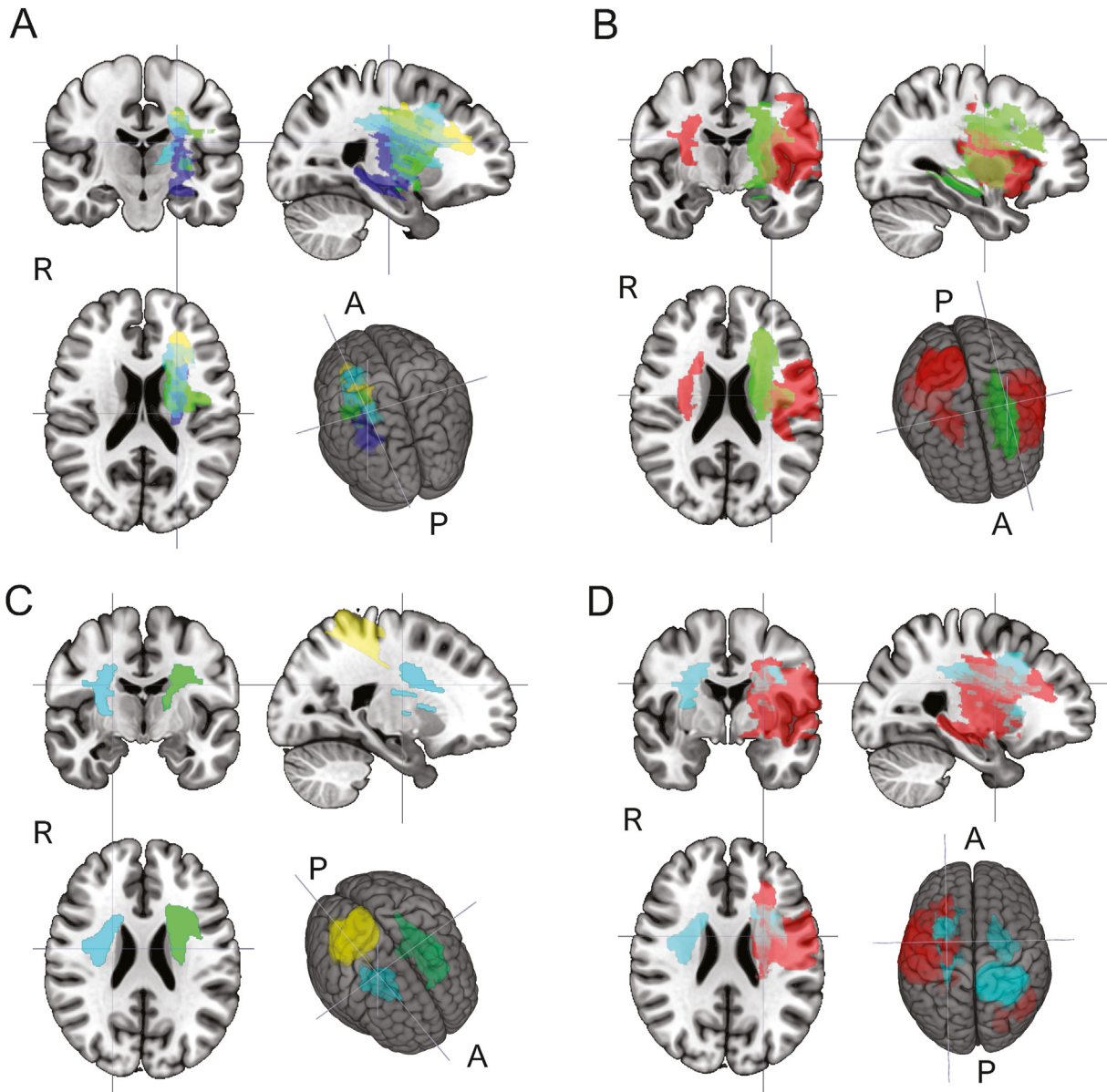


Fig. 3 – Stroke lesions of the participants. A. Illustration of individual normalized lesions of patients #7, #9, #11 and #15 (respectively in green, yellow, blue and cyan) leading to impaired spatial organization/angular distortion or hand metrics in TACTILE-TARGET condition. B. Cumulated lesions of patients with TACTILE-TARGET alterations (in green) versus cumulated lesion of all patients without alterations of TACTILE-TARGET representation structure (red). C. Individual normalized lesions of patients #6, #12 and #15 (respectively in blue, yellow and green) leading to impaired spatial organization/angular distortion or hand metrics of ANATOMICAL-TARGET. D. Cumulated lesions of patients with ANATOMICAL-TARGET alterations (cyan) versus cumulated lesion of all patients without alterations (red).

Table 4 – Results of LSM for TACTILE-TARGET condition.

ATLAS	Region	Hand width	Finger length	Organization score	Angular dev.
Brodmann area	BA9 – dorsolateral prefrontal cortex (DLPFC) (left)	–	–	$z = -2.8920451^{B2, \text{ only}}$ $r = -.85$	$z = 3.8727660^{B2}$ $r = .95$
	BA32 – dorsal anterior cingulate cortex (dACC) (left)	–	–	$z = -3.2397133^{B2}$ $r = -.89$	$z = 3.6927833^{B2}$ $r = .93$
	BA46 – dorsolateral prefrontal cortex (DLPFC) (left)	–	–	$z = -3.2119096^{B2\&3}$ $r = -.89$	$z = 3.8469240^{B2\&3}$ $r = -.95$
JHU	Anterior corona radiata (left)	–	–	$z = -3.7636862^{B2\&3}$ $r = -.91$	$z = 3.5921279^{B2\&3, \text{ only}}$ $r = -.93$

Only significant correlations using permutation tests between evaluations and atlas regions are presented, indicated by the presence of a z value and a Pearson r coefficient. In bold, results that are still significant when the region taken into account for LSM computation has ≥ 3 patients with voxels affected (instead of ≥ 2 , see method section). Significant correlations based on more conservative Bonferroni correction based on ≥ 2 patients with voxel affected are indicated with ^{B2} and ≥ 3 patients with ^{B3}; the superscript ^{only} indicates that the correlation was significant only with Bonferroni correction.

No significant correlation was found for *Hand width* and *Finger length*. Finally, lesions of left anterior corona radiata were associated with *Organization score*. All correlations found between lesion site and *Organization score* or with *Angular deviation* pointed in the same direction: the more severe the lesion, the more distorted the tactile representation, resulting in a lower *Organization score* and a greater *Angular deviation*.

No significant LSM correlation was found for the ANATOMICAL-TARGET condition: Fig. 3C and D illustrate the heterogeneous lesions of patients showing alterations of hand representation in the ANATOMICAL-TARGET condition.

4. Discussion

The first aim of this study was to identify potential alterations of the spatial representations of the affected hand in hemiparetic stroke patients. A few single-case reports anecdotally reported disturbed somatotopic organization and localization in some patients after stroke (Birznieks et al., 2012; Rapp et al., 2002; Rinderknecht et al., 2019; van Stralen et al., 2011). Since the spatial representation of the hand is closely related to the ability to plan and execute movements, our hypothesis was that the hand representation will be related to motor deficits after stroke. Based on four spatial evaluations of hand representations (two metrics and two structural measures) obtained in this prospective study involving a substantial sample, we found that at least one value of these four variables occurred outside the normal range in approximately half of the sample, indicating potentially altered hand representation of the impaired limb. Quantitatively, 65% (13/20) of the patients had at least one abnormal value, in the TACTILE-TARGET condition, and 45% (9/20) in the ANATOMICAL-TARGET condition.

Our second aim was to relate the characteristics of the spatial representation to the post-stroke clinical motor (or sensory) deficits. We found that changes in hand metrics (hand width and finger length) significantly correlated with the motor deficits: a larger hand representation was associated with more severe motor deficits. Furthermore, hand metrics correlated with performance in the Moberg Pick Up test, which assesses precision grip function, while the two structural measures (spatial organization and angular distortion) did not correlate with clinical motor assessments. In addition, no correlation was found between alterations in

spatial representation and clinical sensory assessment, indicating that the changes in spatial coding were not solely due to sensory integration deficits but to higher-order sensory processing impairments.

Our third aim was to explore the localization of lesions corresponding to deficits in the TACTILE-TARGET or ANATOMICAL-TARGET spatial representations. Through lesion-symptom mapping (LSM), and despite the small sample, we found significant correlations specifically between the two structural measures of tactile spatial representation and several lesioned areas: Brodmann areas 9, 32, and 46, as well as the anterior corona radiata.

4.1. Changes in hand representation related to motor performances

In a previous study involving healthy participants (Dupin et al., 2021), we found that the metrics of spatial hand representations (under tactile and anatomical conditions) undergo shrinkage over the lifespan. This reduction in the size of the hand (implicit body) representation was found to start during childhood (Cardinali et al., 2019; Van der Looven et al., 2021), suggesting the presence of a common mechanism, possibly related to optimization or plasticity of hand function. This is coherent with findings of shrinking hand representations in individuals with motor expertise (Coelho et al., 2019; Mora et al., 2021), who undergo long-term and intensive sensorimotor learning. It is also consistent with the fact that metric distortions are found both for action and perception (Peviani & Bottini, 2018).

In the present study, the correlations between hand representation metrics and motor assessments were consistent: good motor performance of the paretic limb was correlated with smaller hand representations. However, the causal link needs to be determined: the larger hand may be caused by the motor impairment itself or by a commonly lesioned area. Another possibility is that a larger hand may be related to intensive rehabilitation and/or plasticity processes in hand function as suggested by previous studies (Coelho et al., 2019; Dupin et al., 2021; Mora et al., 2021; Van der Looven et al., 2021), where a childhood learning/plasticity phase corresponds to larger hand representations, while expertise leads to smaller hand representations. A longitudinal study, assessing hand representations during the acute phase after

stroke, and then during the chronic phase and rehabilitation, may provide an answer.

Spatial structure did not show significant correlation with motor assessment, however the structure of tactile and anatomical representation were independently affected in a part of the patients, indicating possibly a direct effect of the lesion contrary to change in metrics that could be related to motor function.

4.2. Shift in general localization

Similarly to previous case reports, we found a proximal shift of the hand after stroke (Rapp et al., 2002; Rinderknecht et al., 2019). However this shift was not different between in paretic and non-paretic hands in both TACTILE- and ANATOMICAL-TARGET conditions and a similar pattern was also found in controls. This shift mostly relies on the shift of the nails. It is consequently difficult to distinguish a shift of the hand from a change in finger length or a combination of the two. Our results extend findings concerning hand shift of tactile spatial coding to shift of implicit body representation, both correlated (Supplementary Fig. 2), indicating a common substrate between shift in tactile and body representations.

4.3. Difference between hand metrics and spatial structure

Behavioral analysis as well as lesion-symptom mapping showed that hand metrics and spatial structural measures (angular deviation and organization) seem to capture different representational aspects. Firstly, clinical motor assessments

correlated with hand metrics, but not with structural measures. Secondly, hand width and finger length correlated between conditions (TACTILE- and ANATOMICAL-TARGET), indicating common underlying mechanisms, contrary to the complete absence of correlation for structural organization (see Supplementary Table 1). Moreover, tactile metrics correlate with tactile structure and similarly, anatomical metrics correlates with corresponding structure (see Supplementary Table 1) which also indicate specific factor of metrics for tactile and body spatial representation.

Together, these results suggest that the mechanisms influencing or affecting hand metrics and structural measures of the hand representation are partially different, and that structural measures (but not metrics) of body and tactile spatial representations rely on different mechanisms.

As the patients' general location of the hand representation was similar between conditions (TACTILE-TARGET vs ANATOMICAL-TARGET, see Supplementary Fig. 2 for correlations and comparison between conditions) and not specifically affected by the impaired motor hand and independently from whether the structure was impaired or not (see also Supplementary Fig. 1). The affected tactile structural organization may correspond to how tactile information is mapped over this more global body representation (characterized by location and metrics). This would indicate at least four different processing steps: (1) global body (-part) representation (location and metrics), (2) Specific metrics for touch and body (3) how touch is mapped over the global body location; and (4) how fine body representation (fingers) is mapped over the global body (hand) location. These distinctions are described in Fig. 4.

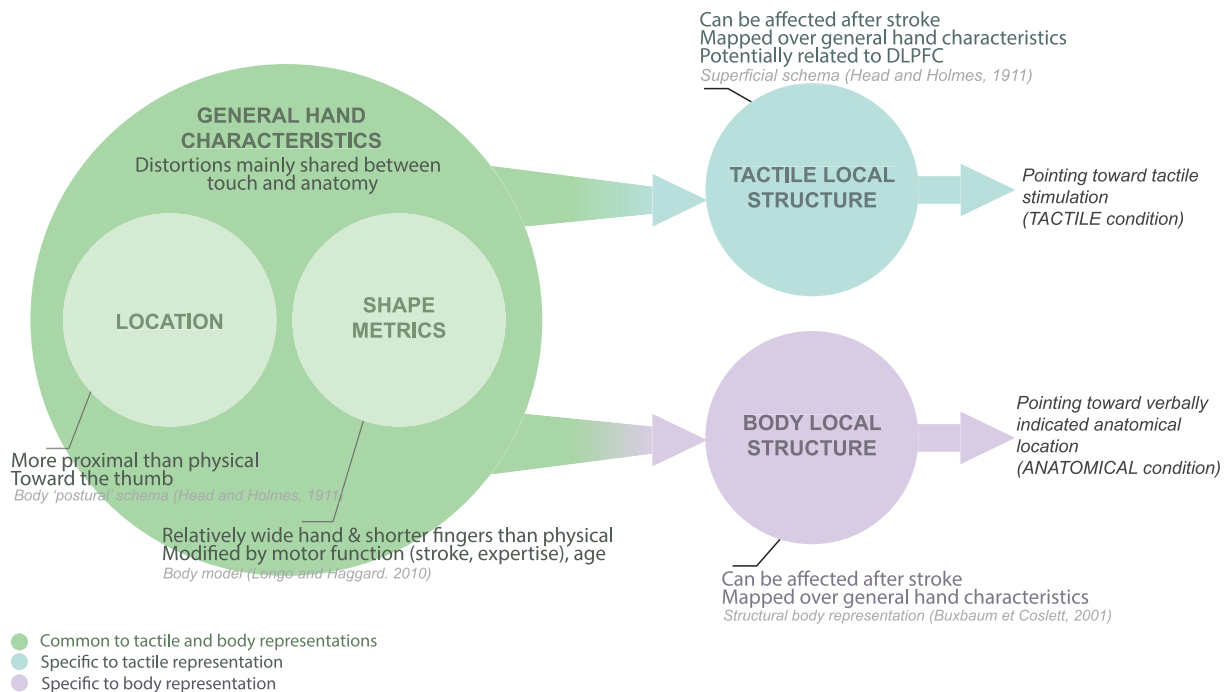


Fig. 4 – Schematic summary of results. The different measures (circles) organized by their characteristics and linked with theoretical concept of body and tactile representations they are close to (light gray, italic).

4.4. Spatial structure alteration and lesion-symptom mapping

In our preliminary LSM analysis, altered structural measures (organization score, angular deviation) of TACTILE-TARGET condition correlated with lesions located in prefrontal cortex, in BA32 and BA46. Areas 46 (and 9, which only correlated with angular deviation), are subdivisions of the dorsolateral prefrontal cortex (DLPFC), and area 32 forms part of the anterior cingulate cortex. These areas are functionally and anatomically interconnected (Jung et al., 2022), and are also connected to the posterior parietal cortex (PPC), i.e., to BA7 and to primary somatosensory cortex (Jung et al., 2022; Rolls et al., 2023), which are involved in somatosensory processing (Bolton et al., 2012; Noel et al., 2022; Rolls et al., 2023). DLPFC is part of the network processing multimodal (visuo-tactile) spatial representations for spatial working memory that also involves anterior cingulate cortex (including BA32/dACC) (Banati et al., 2000; Ricciardi et al., 2006) where information is coded in a non-somatotopic reference frame. Additionally, DLPFC has been found to play a specific role in the spatial representation of sensory targets for action purpose (Goldman-Rakic et al., 1992; Mars & Grol, 2007). Consequently, the impaired function assessed in structural distortion of touch in our task may potentially concern the coding of tactile information in external space necessary for action control, consisting here in a pointing movement. Additional evidence for the role of DLPFC for dynamic spatial body representation arises from lesion studies that have shown impairments in tasks involving on-line coding of posture to lesions in DLPFC and parietal cortex (Schwoebel & Coslett, 2005). However, the involvement of DLPFC in tactile remapping and external spatial coding of somatosensory information has not yet been elucidated.

4.5. Limitations of the study

Participants were assessed once and during the chronic phase which limits the interpretation of altered representations: hand metrics could be related to more intense and/or prolonged rehabilitation for patients with more severe deficits. However, in this case, this assessment could also be useful to understand the plasticity of hand representation during rehabilitation. Another limitation is the small number of participants ($N = 9$) who underwent MRI and were included in the lesion symptom analysis. Despite the different statistical methods used to maximize their robustness, LSM results should be confirmed in a larger sample. Whether left and right hemisphere lesions produce homologous alterations in hand representation needs further investigation since only one patient with MRI had right hemisphere lesion. Finally, these results were obtained with a static target hand and whether properties, such as larger hand representations relating to more severe motor deficits, pertain to moving (dynamic) situations remains to be explored.

4.6. Conclusion

In approximately 50% of patients with persistent upper limb hemiparesis post-stroke, either the anatomical or the tactile spatial representations of the hand were affected. Importantly, no correlation was found between alterations in hand

representation and deficient light touch sensitivity, excluding a purely somatosensory origin for these distortions. Patients exhibited larger spatial hand representations for both their paretic and non-paretic hands, and this increase correlated with the severity of their motor deficits, suggesting a common neural substrate for the metrics of the left and right hand representations, independent of the tactile/anatomical condition. This change in hand metrics might reflect a direct post-stroke alteration or manifest mechanisms of learning and/or plasticity. While further studies will be necessary to understand the cause of changes in hand metrics, a potential ramification concerns upper limb post-stroke rehabilitation and plasticity targeting the spatial hand representation. Lesions in the dorsolateral prefrontal cortex were associated with deficits in the spatial organization of tactile representation, which should be confirmed in a larger number of patients. Finally, while changes in hand metrics and global localization occurred simultaneously in tactile and anatomical spatial representations, alterations in spatial organization occurred independently between the two representations. This suggests that some characteristics share common mechanisms (reflected by common metrics and location), while others are distinct (such as spatial structure) between body (anatomical) and tactile spatial representations.

Funding

This work was supported by the French Stroke Research Foundation (Fondation pour la Recherche sur les AVC, grant number FRAVC170922008). LD was supported by a grant from Fondation Pierre Deniker (Fondation de l'Avenir, grant number FS-MAT-17), and Project RHU PsyCARE, (grant number ANR-18-RHUS-0014).

Open practices

The study in this article has earned Open Materials badges for transparent practices. The materials studies are available at: <https://doi.org/10.17632/yzp6vkzt29.1>.

CRediT authorship contribution statement

Lucile Dupin: Writing – review & editing, Writing – original draft, Visualization, Software, Methodology, Investigation, Formal analysis, Conceptualization. **Eloïse Gerardin:** Writing – review & editing, Investigation. **Maxime Térémetz:** Investigation. **Sonia Hamdoun:** Resources. **Guillaume Turc:** Resources. **Marc A. Maier:** Writing – review & editing, Conceptualization. **Jean-Claude Baron:** Writing – review & editing, Resources. **Pável G. Lindberg:** Writing – review & editing, Validation, Supervision, Funding acquisition, Conceptualization.

Declaration of competing interest

None.

Supplementary data

Supplementary data to this article can be found online at <https://doi.org/10.1016/j.cortex.2024.04.015>.

REFERENCES

- Banati, R. B., Goerres, G. W., Tjoa, C., Aggleton, J. P., & Grasby, P. (2000). The functional anatomy of visual-tactile integration in man: A study using positron emission tomography. *Neuropsychologia*, 38(2), 115–124. [https://doi.org/10.1016/S0028-3932\(99\)00074-3](https://doi.org/10.1016/S0028-3932(99)00074-3)
- Birnieks, I., Logina, I., & Wasner, G. (2012). Somatotopic mismatch following stroke: A pathophysiological condition escaping detection. *BMJ Case Reports*. <https://doi.org/10.1136/bcr-2012-006304>
- Bolton, D. A. E., Brown, K. E., McIlroy, W. E., & Staines, W. R. (2012). Transient inhibition of the dorsolateral prefrontal cortex disrupts somatosensory modulation during standing balance as measured by electroencephalography. *NeuroReport*, 23(6), 369–372. <https://doi.org/10.1097/WNR.0b013e328352027c>
- Brandes, J., & Heed, T. (2015). Reach trajectories characterize tactile localization for sensorimotor decision making. *The Journal of Neuroscience*, 35(40), 13648–13658. <https://doi.org/10.1523/JNEUROSCI.1873-14.2015>
- Brodmann, K. (1909). *Vergleichende Lokalisationslehre der Grosshirnrinde in ihren Prinzipien dargestellt auf Grund des Zellenbaues*.
- Caggiano, P., & Cocchini, G. (2020). The functional body: Does body representation reflect functional properties? *Experimental Brain Research*, 238(1), 153–169. <https://doi.org/10.1007/s00221-019-05705-w>
- Cardinali, L., Serino, A., & Gori, M. (2019). Hand size underestimation grows during childhood. *Scientific Reports*, 9(1), 1–8. <https://doi.org/10.1038/s41598-019-49500-7>
- Cataldo, A., Dupin, L., Dempsey-Jones, H., Gomi, H., & Haggard, P. (2022). Interplay of tactile and motor information in constructing spatial self-perception. *Current Biology*, 32(6), 1301–1309.e3.
- Cataldo, A., Dupin, L., Gomi, H., & Haggard, P. (2021). Sensorimotor signals underlying space perception: An investigation based on self-touch. *Neuropsychologia*, 151, Article 107729. <https://doi.org/10.1016/j.neuropsychologia.2020.107729>
- Cheverud, J. M. (2001). A simple correction for multiple comparisons in interval mapping genome scans. *Heredity*, 87(1), 52–58. <https://doi.org/10.1046/j.1365-2540.2001.00901.x>
- Coelho, L. A., Schacher, J. P., Scammel, C., Doan, J. B., & Gonzalez, C. L. R. (2019). Long- but not short-term tool-use changes hand representation. *Experimental Brain Research*, 237(1), 137–146. <https://doi.org/10.1007/s00221-018-5408-y>
- Cohen, Y. E., & Andersen, R. A. (2002). A common reference frame for movement plans in the posterior parietal cortex. *Nature Reviews Neuroscience*, 3(7), 553–562. <https://doi.org/10.1038/nrn873>
- Derringer, J. (2018). A simple correction for non-independent tests. *PsyArXiv*. <https://doi.org/10.31234/OSF.IO/F2TYW>
- Dupin, L., Cuenca, M., Baron, J.-C., Maier, M. A., & Lindberg, P. G. (2021). Shrinking of spatial hand representation but not of objects across the lifespan. *Cortex; a Journal Devoted to the Study of the Nervous System and Behavior*, 146, 173–185. <https://doi.org/10.1016/j.cortex.2021.10.009>
- Dupin, L., Hayward, V., & Wexler, M. (2015). Direct coupling of haptic signals between hands. *Proceedings of the National Academy of Sciences of the United States of America*, 112(2), 619–624. <https://doi.org/10.1073/pnas.1419539112>
- Dupin, L., Hayward, V., & Wexler, M. (2017). Generalized movement representation in haptic perception. *Journal of Experimental Psychology: Human Perception and Performance*, 43(3), 581. <https://doi.org/10.1037/xhp0000327>
- Dupin, L., Hayward, V., & Wexler, M. (2018). Radial trunk-centred reference frame in haptic perception. *Scientific Reports*, 8(1), Article 13550. <https://doi.org/10.1038/s41598-018-32002-3>
- Goldman-Rakic, P. S., Bates, J. F., & Chafee, M. V. (1992). The prefrontal cortex and internally generated motor acts. *Current Opinion in Neurobiology*, 2(6), 830–835. [https://doi.org/10.1016/0959-4388\(92\)90141-7](https://doi.org/10.1016/0959-4388(92)90141-7)
- Haggard, P., Kitadono, K., Press, C., & Taylor-Clarke, M. (2006). The brain's fingers and hands. *Experimental Brain Research*, 172(1), 94–102. <https://doi.org/10.1007/s00221-005-0311-8>
- Head, H., & Holmes, G. (1911). Sensory disturbances from cerebral lesions. *Brain: a Journal of Neurology*, 34(2–3), 102–254. <https://doi.org/10.1093/BRAIN/34.2-3.102>
- Jung, J. Y., Lambon Ralph, M. A., & Jackson, R. L. (2022). Subregions of DLPFC display graded yet distinct structural and functional connectivity. *Journal of Neuroscience*, 42(15), 3241–3252. <https://doi.org/10.1523/JNEUROSCI.1216-21.2022>
- Longo, M. R., Azañón, E., & Haggard, P. (2010). More than skin deep: Body representation beyond primary somatosensory cortex. *Neuropsychologia*, 48(3), 655–668. <https://doi.org/10.1016/j.neuropsychologia.2009.08.022>
- Longo, M. R., & Haggard, P. (2010). An implicit body representation underlying human position sense. *Proceedings of the National Academy of Sciences of the United States of America*, 107(26), 11727–11732. <https://doi.org/10.1073/pnas.1003483107>
- Longo, M. R., Mattioni, S., & Ganea, N. (2015). Perceptual and conceptual distortions of implicit hand maps. *Frontiers in Human Neuroscience*, 9(DEC), 656. <https://doi.org/10.3389/fnhum.2015.00656>
- Lyle, R. C. (1981). A performance test for assessment of upper limb function in physical rehabilitation treatment and research. *International Journal of Rehabilitation Research*, 4(4), 483–492. <https://doi.org/10.1097/00004356-198112000-00001>
- Mars, R. B., & Grol, M. J. (2007). Dorsolateral prefrontal cortex, working memory, and prospective coding for action. *Journal of Neuroscience*, 27(8), 1801–1802. <https://doi.org/10.1523/JNEUROSCI.5344-06.2007>. Society for Neuroscience.
- Mathiowetz, V., Volland, G., Kashman, N., & Weber, K. (1985). Adult norms for the box and block test of manual dexterity. *The American Journal of Occupational Therapy: Official Publication of the American Occupational Therapy Association*, 39(6), 386–391. <http://www.ncbi.nlm.nih.gov/pubmed/3160243>.
- Medina, J., & Coslett, H. B. (2016). What can errors tell us about body representations? *Cognitive Neuropsychology*, 33(1–2), 5–25. <https://doi.org/10.1080/02643294.2016.1188065>. Routledge.
- Meyer, S., De Bruyn, N., Lafosse, C., Van Dijk, M., Michielsen, M., Thijs, L., Truyens, V., Oostra, K., Krumlinde-Sundholm, L., Peeters, A., Thijs, V., Feys, H., & Verheyden, G. (2016). Somatosensory impairments in the upper limb poststroke. *Neurorehabilitation and Neural Repair*, 30(8), 731–742. <https://doi.org/10.1177/1545968315624779>
- Meyer, S., Karttunen, A. H., Thijs, V., Feys, H., & Verheyden, G. (2014). How do somatosensory deficits in the arm and hand relate to upper limb impairment, activity, and participation problems after stroke? A systematic review. *Physical Therapy*, 94(9), 1220–1231. <https://doi.org/10.2522/ptj.20130271>
- Moberg, E. (1958). Objective methods for determining the functional value of sensibility in the hand. *The Journal of Bone and Joint Surgery. British Volume*, 40-B(3), 454–476. <https://doi.org/10.1302/0301-620X.40B3.454>
- Mora, L., Sedda, A., Esteban, T., & Cocchini, G. (2021). The signing body: Extensive sign language practice shapes the size of hands and face. *Experimental Brain Research*, 239(7), 2233–2249. <https://doi.org/10.1007/s00221-021-06121-9>

- Mori, S., Susumu, & Crain, B. J. (2005). *MRI atlas of human white matter*. Elsevier.
- Noel, J. P., Balzani, E., Avila, E., Lakshminarasimhan, K., Bruni, S., Adefantis, P., Savin, C., & Angelaki, D. E. (2022). Coding of latent variables in sensory, parietal, and frontal cortices during closed-loop virtual navigation. *eLife*, 11, 1–54. <https://doi.org/10.7554/eLife.80280>
- Nyholt, D. R. (2004). A simple correction for multiple testing for single-nucleotide polymorphisms in linkage disequilibrium with each other. *American Journal of Human Genetics*, 74(4), 765–769. <https://doi.org/10.1086/383251>
- Peviani, V., & Bottini, G. (2018). The distorted hand metric representation serves both perception and action. *Journal of Cognitive Psychology*, 30(8), 880–893. <https://doi.org/10.1080/20445911.2018.1538154>
- Plantin, J., Verneau, M., Godbolt, A. K., Pennati, G. V., Laurencikas, E., Johansson, B., Krumlinde-Sundholm, L., Baron, J. C., Borg, J., & Lindberg, P. G. (2021). Recovery and prediction of bimanual hand use after stroke. *Neurology*, 97(7), E706–E719. <https://doi.org/10.1212/WNL.00000000000012366>
- Ramsey, L. E., Siegel, J. S., Lang, C. E., Strube, M., Shulman, G. L., & Corbetta, M. (2017). Behavioural clusters and predictors of performance during recovery from stroke. *Nature Human Behaviour*, 1(3). <https://doi.org/10.1038/s41562-016-0038>
- Rapp, B., Hendel, S. K., & Medina, J. (2002). Remodeling of somatosensory hand representations following cerebral lesions in humans. *NeuroReport*, 13(2), 207–211. <https://doi.org/10.1097/00001756-200202110-00007>
- Ricciardi, E., Bonino, D., Gentili, C., Sani, L., Pietrini, P., & Vecchi, T. (2006). Neural correlates of spatial working memory in humans: A functional magnetic resonance imaging study comparing visual and tactile processes. *Neuroscience*, 139(1), 339–349. <https://doi.org/10.1016/j.neuroscience.2005.08.045>
- Rinderknecht, M. D., Dueñas, J. A., Held, J. P., Lamberg, O., Conti, F. M., Zizlsperger, L., Luft, A. R., Hepp-Reymond, M.-C., & Gassert, R. (2019). Automated and quantitative assessment of tactile mislocalization after stroke. *Frontiers in Neurology*, 10(JUN), 593. <https://doi.org/10.3389/fneur.2019.00593>
- Rolls, E. T., Deco, G., Huang, C. C., & Feng, J. (2023). Prefrontal and somatosensory-motor cortex effective connectivity in humans. *Cerebral Cortex*, 33(8), 4939–4963. <https://doi.org/10.1093/cercor/bhac391>
- Schwobed, J., & Coslett, H. B. (2005). Evidence for multiple, distinct representations of the human body. *Journal of Cognitive Neuroscience*, 17(4), 543–553. <https://doi.org/10.1162/0898929053467587>
- Tamè, L., Bumpus, N., Linkenauger, S. A., & Longo, M. R. (2017). Distorted body representations are robust to differences in experimental instructions. *Attention, Perception, and Psychophysics*, 79(4), 1204–1216. <https://doi.org/10.3758/s13414-017-1301-1>
- Taub, E., Miller, N. E., Novack, T. A., Cook, E. W., Fleming, W. C., Nepomuceno, C. S., Connell, J. S., & Crago, J. E. (1993). Technique to improve chronic motor deficit after stroke. *Archives of Physical Medicine and Rehabilitation*, 74(4), 347–354. <https://europepmc.org/article/MED/8466415>
- Van der Looven, R., Deschrijver, M., Hermans, L., De Muynck, M., & Vingerhoets, G. (2021). Hand size representation in healthy children and young adults. *Journal of Experimental Child Psychology*, 203, Article 105016. <https://doi.org/10.1016/j.jecp.2020.105016>
- van Stralen, H. E., van Zandvoort, M. J. E., & Dijkerman, H. C. (2011). The role of self-touch in somatosensory and body representation disorders after stroke. *Philosophical Transactions of the Royal Society B: Biological Sciences*, 366(1581), 3142–3152. <https://doi.org/10.1098/rstb.2011.0163>. Royal Society.
- Verbe, J., Lindberg, P. G., Gorwood, P., Dupin, L., & Duriez, P. (2021). Spatial hand representation in anorexia nervosa: A controlled pilot study. *Scientific Reports*, 11(1), Article 19724. <https://doi.org/10.1038/s41598-021-99101-6>
- Wakana, S., Caprihan, A., Panzenboeck, M. M., Fallon, J. H., Perry, M., Gollub, R. L., Hua, K., Zhang, J., Jiang, H., Dubey, P., Blitz, A., van Zijl, P., & Mori, S. (2007). Reproducibility of quantitative tractography methods applied to cerebral white matter. *NeuroImage*, 36(3), 630–644. <https://doi.org/10.1016/j.neuroimage.2007.02.049>
- Weinstein, S. (1993). Fifty years of somatosensory research: From the Semmes-Weinstein monofilaments to the Weinstein enhanced sensory test. *Journal of Hand Therapy*, 6(1), 11–22. [https://doi.org/10.1016/S0894-1130\(12\)80176-1](https://doi.org/10.1016/S0894-1130(12)80176-1)
- Zandvliet, S. B., Kwakkel, G., Nijland, R. H. M., van Wegen, E. E. H., & Meskers, C. G. M. (2020). Is recovery of somatosensory impairment conditional for upper-limb motor recovery early after stroke? *Neurorehabilitation and Neural Repair*, 34(5), 403–416. <https://doi.org/10.1177/1545968320907075>